Journal of Orthopaedic Translation 46 (2024) 116–128

Contents lists available at ScienceDirect

Journal of Orthopaedic Translation

journal homepage: www.journals.elsevier.com/journal-of-orthopaedic-translation

Original Article

SPARCL1 promotes chondrocytes extracellular matrix degradation and inflammation in osteoarthritis via TNF/NF-κB pathway

Yu Miao [a,b,1], Shenghui Wu [a,b,1], Ziling Gong [a,b,1], Yiwei Chen [a,b], Feng Xue [a,b], Kexin Liu [a,b], Jian Zou [a], Yong Feng [a,b,**], Guangyi Li [a,b,*]

[a] Department of Orthopaedics, Shanghai Jiao Tong University Affiliated Sixth People's Hospital, No.600, Yishan Road, Shanghai, 200233, China
[b] Institute of Microsurgery on Extremities, Shanghai Jiao Tong University Affiliated Sixth People's Hospital, Shanghai, 200233, China

ARTICLE INFO

Keywords:
ECM degradation
Osteoarthritis
SPARCL1
TNF/NF-κB

ABSTRACT

Objectives: SPARCL1 is a matricellular protein that mediates the cell–matrix interactions and participates in physiological processes such as cell adhesion, differentiation and proliferation. However, its role in chondrocyte and osteoarthritis (OA) progression has not been fully characterized. We aimed to evaluate the effects of SPARCL1 on OA through in vitro and *in vivo* experiments.

Methods: Expression of SPARCL1 was examined in 55 paired human OA samples. Effects of Sparcl1 on chondrocytes were identified in vitro. Intra-articular injection was performed in an anterior cruciate ligament transection (ACLT) mouse model. Alterations of SPARCL1-mediated signaling pathway were identified by RNA-seq analysis. qPCR and western-blot were used to demonstrate the potential signaling pathway.

Results: SPARCL1 expression in the OA cartilage was increased compared with undamaged cartilage. Recombinant Sparcl1 protein induced extracellular matrix degradation in chondrocytes. Furthermore, intra-articular injection of recombinant Sparcl1 protein in ACLT mice could promote OA pathogenesis. Mechanistically, Sparcl1 activated TNF/NF-κB pathway and consequently led to increased transcription of inflammatory factors and catabolism genes of cartilage, which could be reversed by NF-κB inhibitor BAY 11–7082.

Conclusion: SPARCL1 could promote extracellular matrix degradation and inflammatory response to accelerate OA progression via TNF/NF-κB pathway.

The translational potential of this article: The current research could help to gain further insights into the underlying molecular mechanism in OA development, and provides a biological rationale for the use of SPARCL1 as a potential therapeutic target of OA.

The translational potential of this article

The current research could help to gain further insights into the underlying molecular mechanism in OA development, and provides a biological rationale for the use of SPARCL1 as a potential therapeutic target of OA.

1. Introduction

Osteoarthritis (OA) is the most common joint disease worldwide, and is characterized by pain and functional impairment [1]. OA progression is closely related to inflammatory, mechanical, and metabolic factors [2], which may ultimately lead to structural destruction, including articular cartilage, subchondral bone, synovium, joint capsule, ligaments and periarticular muscles [3,4]. Among these destructions, dysfunction of the articular cartilage was considered as a hallmark feature, which provides critical elastic support to disperse pressure and shear stress as joints move [5]. Chondrocytes is the only type of cell in articular cartilage responsible for extracellular matrix (ECM) production [6]. ECM degradation has also been regarded to be closely associated

* Corresponding author. Department of Orthopaedics, Shanghai Jiao Tong University Affiliated Sixth People's Hospital, No.600, Yishan Road, Shanghai 200233, China.
** Corresponding author. Department of Orthopaedics, Shanghai Jiao Tong University Affiliated Sixth People's Hospital, No.600, Yishan Road, Shanghai 200233, China.
E-mail addresses: fengyongxsh@gmail.com (Y. Feng), guangyi.li@shsmu.edu.cn (G. Li).
[1] These authors contributed equally to this work

https://doi.org/10.1016/j.jot.2024.02.009
Received 7 June 2023; Received in revised form 27 November 2023; Accepted 29 February 2024

with OA progression [7]. Therefore, further research on chondrocyte metabolism and ECM degradation may help us better understand OA pathogenesis and progression, which is essential for the development of new treatment strategies.

The secreted protein acidic rich in cysteine-like 1 (SPARCL1), also known as Hevin, MAST9, SC1 and ECM2, is a matricellular protein which is a member of SPARC-related protein family [8]. SPARC family members could be secreted into the ECM and play different roles in regulating cell adhesion, proliferation, metastasis, and growth factor signaling to affect the extracellular matrix (ECM) and interactions between cells [9]. Studies have revealed that SPARCL1 is an adhesion molecule mediating the cell–matrix interactions and participates in physiological processes such as cell adhesion, differentiation and proliferation [10,11]. Multiple studies have revealed the role of SPARCL1 in various cancers, including cervical, colorectal, and ovarian cancer. SPARCL1 could inhibit the proliferation and migration of kidney cancer cells by inactivating the JNK/ERK/p38 pathway [12]. In ovarian cancer, SPARCL1 inhibited cell proliferation and migration by downregulating the MEK/ERK signaling pathway [13]. It also exhibits inhibitory effects on cell motility and cell adhesion in osteosarcoma via activating WNT/β-catenin signaling [14]. Besides tumors, SPARCL1 was reported promoting muscle cell differentiation via BMP7-mediated BMP/TGF-β cell signaling pathway [15]. These results suggest that the biological functions of SPARCL1 are regulated through different signaling pathways in different tissues. In OA, SPARCL1 expression was reported elevated in OA meniscus through RNA microarray study [16], but its expression is still not clear in OA cartilage. Meanwhile, the effects of SPARCL1 on chondrocytes or OA progression and the underlying mechanism remain elusive, despite of its close relationship with ECM.

Overall, the functions of SPARCL1, an important ECM molecule, are not well-understood in OA progression and chondrocytes. Determining the function and mechanism of SPARCL1 in regulating OA progression may have important potential application value for treating OA. In this study, we evaluated the expression of SPARCL1 in OA cartilage and the function of SPARCL1 were also detected. The mechanism about how SPARCL1 affect OA progression were also explored. We concluded that SPARCL1 could promote inflammation and ECM degradation in chondrocytes through Tumor necrosis factor/Nuclear factor-kappa B (TNF/NF-κB) pathway in OA development, and suppression of SPARCL1 may provide a new approach for OA treatment.

2. Materials and methods

2.1. Chemicals, reagents, and antibodies

Details of chemicals, reagents, and antibodies used were listed in Supplementary Table 1.

2.2. Patients and specimens

Articular samples were collected from 55 patients with knee OA who underwent knee arthroplasty surgery. Specimens that included all cartilage layers and subchondral bone were separately harvested, and divided into damaged area (designed as OA) and corresponding undamaged area (designed as Undamaged). Inclusion criteria: OA patients undergoing total knee replacement. Exclusion criteria: 1. Known metabolic or bone related diseases other than OA, such as renal dysfunction, thyroid or parathyroid diseases, malignant tumors, etc.; 2. Other diseases that can affect cartilage structure and quality, such as rheumatoid arthritis; 3. Taking drugs that can affect cartilage and bone metabolism, such as anti-bone resorptive drugs, calcitonin, thyroxine, parathyroid hormone, and sex hormone replacement therapy; 4. History of femoral or tibial osteotomy surgery. All human studies were approved by the ethics committee of Shanghai Sixth People's hospital (Approval Number: 2019-KY-007(K)), and full written consents were obtained before the operative procedure. All the experiments described were carried out in accordance with The Code of Ethics of the World Medical Association (Declaration of Helsinki). Clinical information was collected from patients' records (The characteristics of patients were shown in Supplementary Table 2.).

2.3. Isolation, culture of chondrocytes, and ATDC5 cells

Primary mouse chondrocytes (MCC) were isolated from cartilage fragments, which were dissected from femoral heads, femoral condyles and tibial plateau of C57BL/6 mice. Briefly, articular cartilage was firstly cut into small pieces and digested with 0.25% trypsin at 37 °C for 30 min. After being washed 3 times by PBS, the pieces were fully digested using 0.25% collagenase II at 37 °C for 8 h. Afterwards, the cell suspension was filtered using 70 μm cell strainer and centrifuged (1000 rpm) for 5 min to collect primary chondrocytes. The cells were finally cultured in Dulbecco's modified Eagle's medium (DMEM; HyClone) supplemented with 10% FBS (Gibco) and 1% penicillin/streptomycin cocktail. Chondrocytes at passage 3 were used in this study. ATDC5 cells were cultured in DMEM/F12 (Gibco) containing 5% FBS. ATDC5 cell line has been validated by short tandem repeat (STR) profiling. All cells were maintained in a humidified incubator containing 5% CO2 at 37 °C.

2.4. Cell viability assays and micromass culture

The cell counting kit-8 (CCK-8, Dojindo, Kumamoto, Japan) was used to measure the cell viability. Cells were seeded onto 96-well plates (1,0000 cells per well) and treated with recombinant mouse Sparcl1 protein (R&D Systems Inc.). At proper time, 90 μL of DMEM and 10 μL of CCK-8 were mixed and added to each well and incubated for 2 h at 37 °C. The absorbance at a wavelength of 450 nm was measured on a microplate reader (Mode 680, Bio-Rad, Hercules, USA).

For micromass culture assay, ATDC5 cells were trypsinized, washed and resuspended at 2 × 107 cells/ml in a chondrogenic medium composed of DMEM-F12, 5% FBS, 1 × ITS (Insulin, Transferrin, Selenite) (Sigma Aldrich), recombinant transforming growth factor-β (10 ng/ml), sodium pyruvate, L-proline, ascorbic acid 2-phosphate and dexamethasone. A volume of 10 μl was carefully placed in the center of each well of a 24-well plate. Cells were allowed to adhere for 2 h at 37C, followed by addition of 500 ml chondrogenic medium.

2.5. Experimental post-traumatic OA in mice

Twelve-week-old male wildtype C57BL/6 mice underwent anterior cruciate ligament transection (ACLT) surgery of the right knee to induce mechanical instability and create an experimental OA model. Briefly, after anesthesia with intraperitoneally injection of 0.5% pentobarbital, the anterior cruciate ligament of the right knee was transected. A sham operation was performed without ligament transection. We randomly divided the mice into 3 groups (8 mice in each group): sham-operated mice treated with physiological saline (Sham group), ACLT-operated mice treated with physiological saline (Vehicle group), and ACLT-operated mice treated with recombinant mouse Sparcl1 protein (40 μg/kg) (Sparcl1 group). Mice were given an intra-articular injection of recombinant Sparcl1 protein using 33-gauge needles (Hamilton Company) and 10 μl CASTIGHT syringes (Hamilton Company). Briefly, locate the midpoint of the mouse's patellar tendon by touching, then insert the 33-gauge needle into the joint cavity. When the needle touches the middle ridge of the platform, slightly retract the needle, then perform the injection. The injection was repeated twice a week for 6 consecutive weeks. The right knee was harvested for further evaluation. All animal experiments were approved by the Animal Care and Use Committee of Shanghai Sixth People's Hospital (No. DWLL2022-0539).

2.6. Micro-computerized tomography (Micro-CT) analysis

Briefly, skin and muscles were removed, and the knee joints were

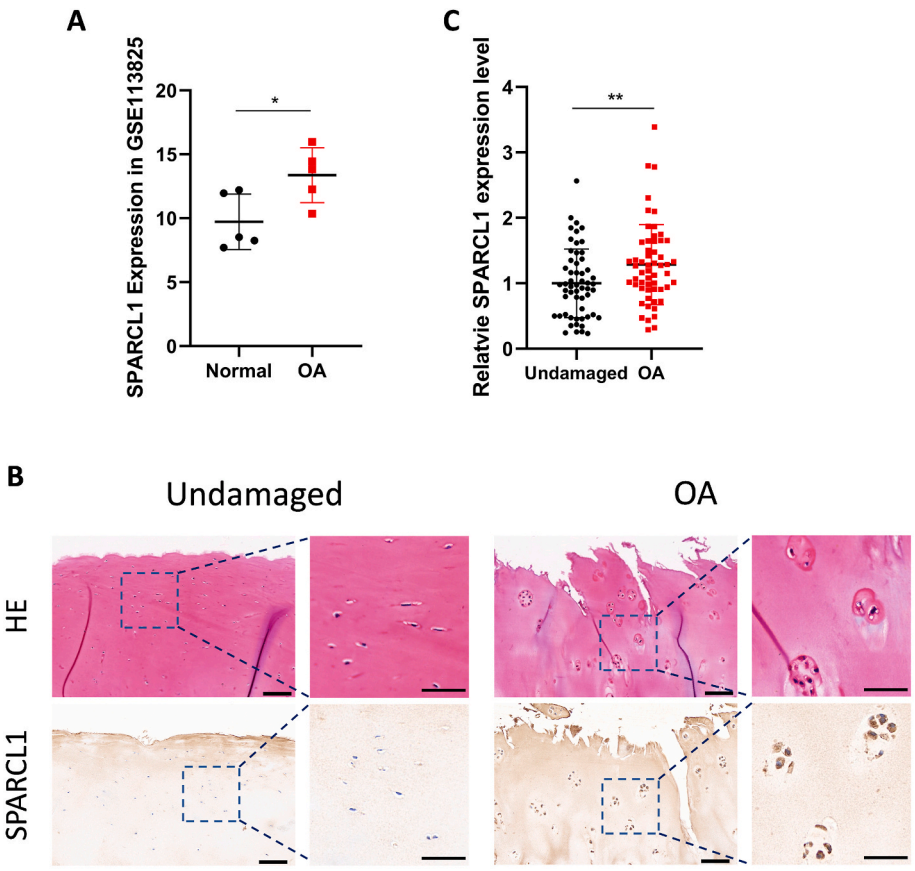

Figure 1. The expression level of SPARCL1 in human OA cartilage. A Microarray profiling analysis data of SPARCL1 expression level in OA cartilage and normal cartilage. Date was originated from GSE113825. Unpaired T-test were used. **B** Immunohistochemistry assay with anti-SPARCL1 in undamaged and OA cartilage tissues. Scale bar, Left, 100 μm; Right, 50 μm. **C** Relative SPARCL1 expression level in OA (n = 55) and corresponding undamaged (n = 55) cartilage tissues based on an immunohistochemistry assay and significance was evaluated by paired Student's t test. Data are expressed as mean ± SD, *P < 0.05; **P < 0.01; ***P < 0.001.

obtained. The joint specimens were then fixed in 4% paraformaldehyde (PFA). All samples were scanned at 9 μm resolution by a micro-CT scanner (SkyScan 1176, Kontich, Belgium). Further analysis was performed with DataViewer (Bruker MicroCT, Kontich, Belgium) and CTAn (Bruker MicroCT, Kontich, Belgium) software. Three-dimensional images were visualized using CTVox software (Bruker MicroCT, Kontich, Belgium). The microarchitecture parameters including bone volume fraction (BV/TV), trabecular number (Tb.N), trabecular thickness (Tb.Th), Bone Surface/Total Volume (BS/TV) Trabecular Bone Separation (Tb.Sp), Trabecular Bone pattern factor (Tb.Pf), Bone Surface/Bone Volume (BS/BV), structure model index (SMI) were analyzed in subchondral and trabecular bone.

2.7. Histology and immunohistochemical assay

Tissues were fixed in 4% paraformaldehyde and subsequently decalcified with buffered EDTA (20% EDTA, pH 7.4). The tissues were embedded in paraffin, sectioned and stained with safranin O/fast green. The cellularity and morphology of cartilage and subchondral bone were examined by experienced histology researchers in a blinded manner using a microscope. The severity of cartilage degeneration of OA model was evaluated by the Osteoarthritis Research Society International (OARSI) scoring system.

For immunohistochemistry (IHC) staining of human samples, sections were heated at 95 °C for 15 min, and then treated with 3% H_2O_2, 0.5% Triton X-100. Nonspecific binding was blocked by 10% bovine serum albumin for 1 h at room temperature. The sections were then incubated with the primary antibody (SPARCL1, 1:100, HUABIO, Cat# ER1917-01) overnight at 4 °C. Finally, the sections were incubated with secondary antibody, counterstained with hematoxylin and visualized by DAB solution for IHC. The immunoreactive level was determined by Image J software.

2.8. Quantitative reverse-transcription PCR (qRT-PCR)

Total RNA from ATDC5 cells and MCCs were extracted using EZ-press RNA Purification Kit (EZBioscience) and quantified by the NanoDrop 2000 spectrophotometer (Thermo, Waltham, USA). Complementary cDNA was synthesized through reverse transcription using a Reverse Transcription Master Mix (EZBioscience). The qPCR assay was performed on QuantStudio 7 (Thermo). Expression levels were normalized to β-actin. The primers were listed in Supplementary Table 3.

2.9. Western blotting

Cells were lysed with RIPA Lysis Buffer added with protease inhibitor and phosphatase inhibitor (Epizyme Biotech). Proteins were separated by 12% SDS polyacrylamide gel electrophoresis (PAGE), and transferred to polyvinylidene fluoride (PVDF) membrane. PVDF membranes were incubated with primary antibodies overnight at 4 °C, incubated with secondary antibodies at room temperature for 1 h, and visualized using the BIO-RAD ChemiDoc XRS + system. Proteins were analyzed with antibodies against matrix metalloproteinases 3 (MMP3) (1:1000, Santa Cruz Cat# sc-21732), ADAMTS5 (1:1 000, Affinity Cat# DF13268), FAK (1:1000, Cell Signaling Technology Cat# 3285), Phospho-FAK (1:1000, Cell Signaling Technology Cat# 3285), NFκB (1:1000, Cell Signaling Technology Cat# 6956), IKKα (1:1000, Cell Signaling Technology Cat#

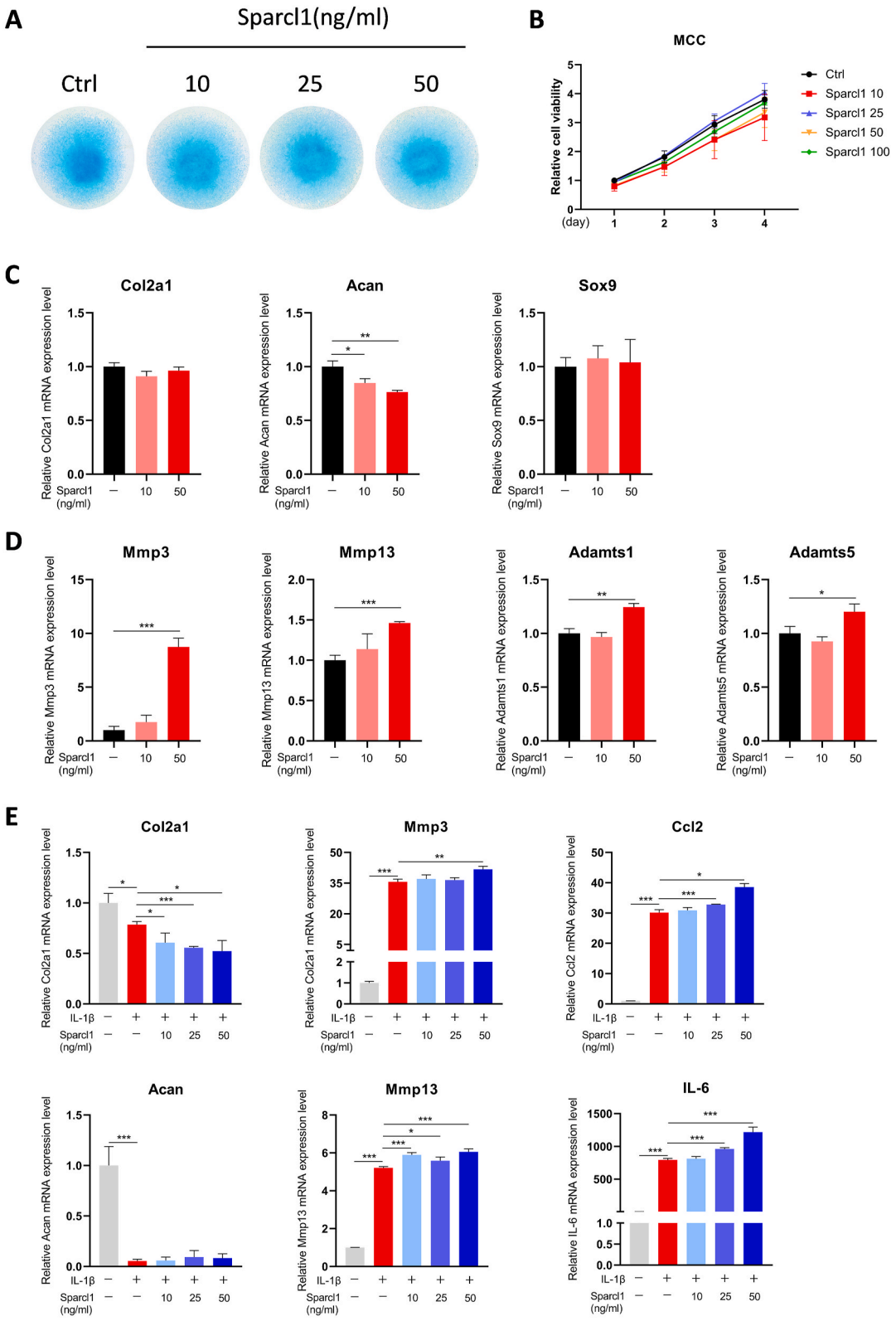

Figure 2. Sparcl1 regulated ECM degradation in chondrocytes. **A** Alcian blue staining of ATDC5 with micromass culture in chondrogenesis media with or without recombinant Sparcl1 protein. Representative image of staining at day 8 is shown. **B** CCK-8 assay test of the cell viability of MCC treated with different concentration of recombinant Sparcl1 protein (10, 25, 50, 100 ng/ml). **C** Quantification of mRNA levels for Col2a1, Acan and Sox9 in MCC treated with recombinant Sparcl1 protein (10 and 50 ng/ml) for 48 h. **D** Quantification of mRNA levels for Mmp3, Mmp13, Adamts1, Adamts5 in MCC treated with recombinant Sparcl1 protein (10 and 50 ng/ml) for 48 h. **E** Quantification of mRNA levels for Col2a1, Acan, Mmp3, Mmp13, Ccl2 and IL-6 in MCC treated with IL-1β (10 ng/ml) and recombinant Sparcl1 protein (10, 25 and 50 ng/ml) for 48 h. Data are expressed as mean ± SD, *P < 0.05; **P < 0.01; ***P < 0.001. One-way ANOVA with post-hoc Bonferroni correction was used for comparisons.

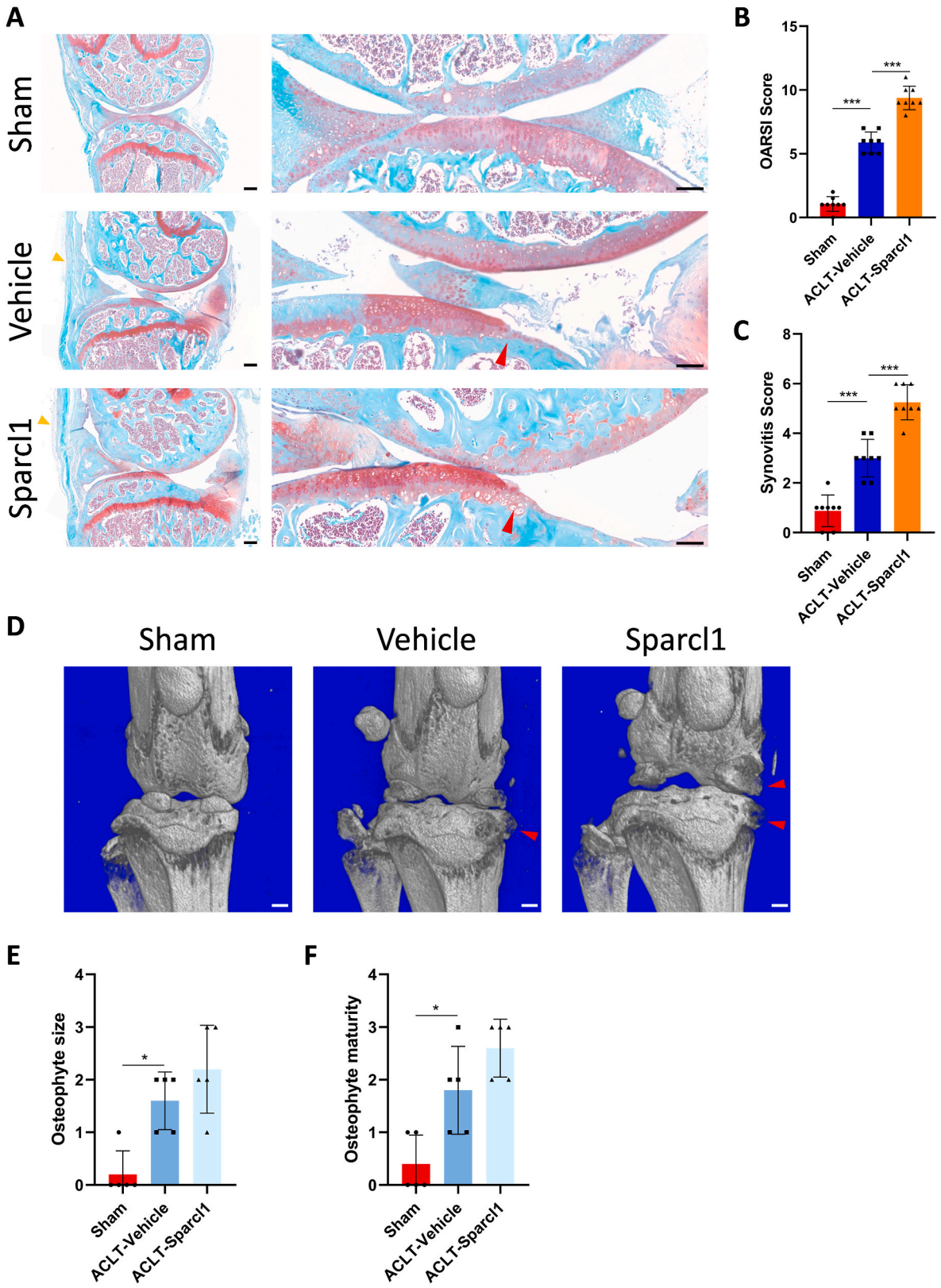

Figure 3. Sparcl1 accelerated OA process in ACLT mice model. A Representative safranin O-fast green images of osteoarthritic knee joints, which were collected 6 weeks after ACLT surgery. Yellow arrowheads indicated articular cartilage degradation. n = 8; Scale bar, left, 200 μm; right, 100 μm. **B** The severity of OA-like phenotype was analyzed using the Osteoarthritis Research Society International (OARSI) score system (n = 8). **C** The degree of synovitis was semi-quantified by the enlargement of synovial lining layers and density of cells (n = 8). **D** Three-dimensional models of mice knee joints. Red arrow showed osteophyte formation. Scale bar, 250 μm. **E, F** Osteophytes were semi-quantified by evaluating the osteophyte formation score consisting of two domains, size (E) and maturity (F) (n = 5) Data are expressed as mean ± SD, *P < 0.05; **P < 0.01; ***P < 0.001. One-way ANOVA with post-hoc Bonferroni correction was used for comparisons.

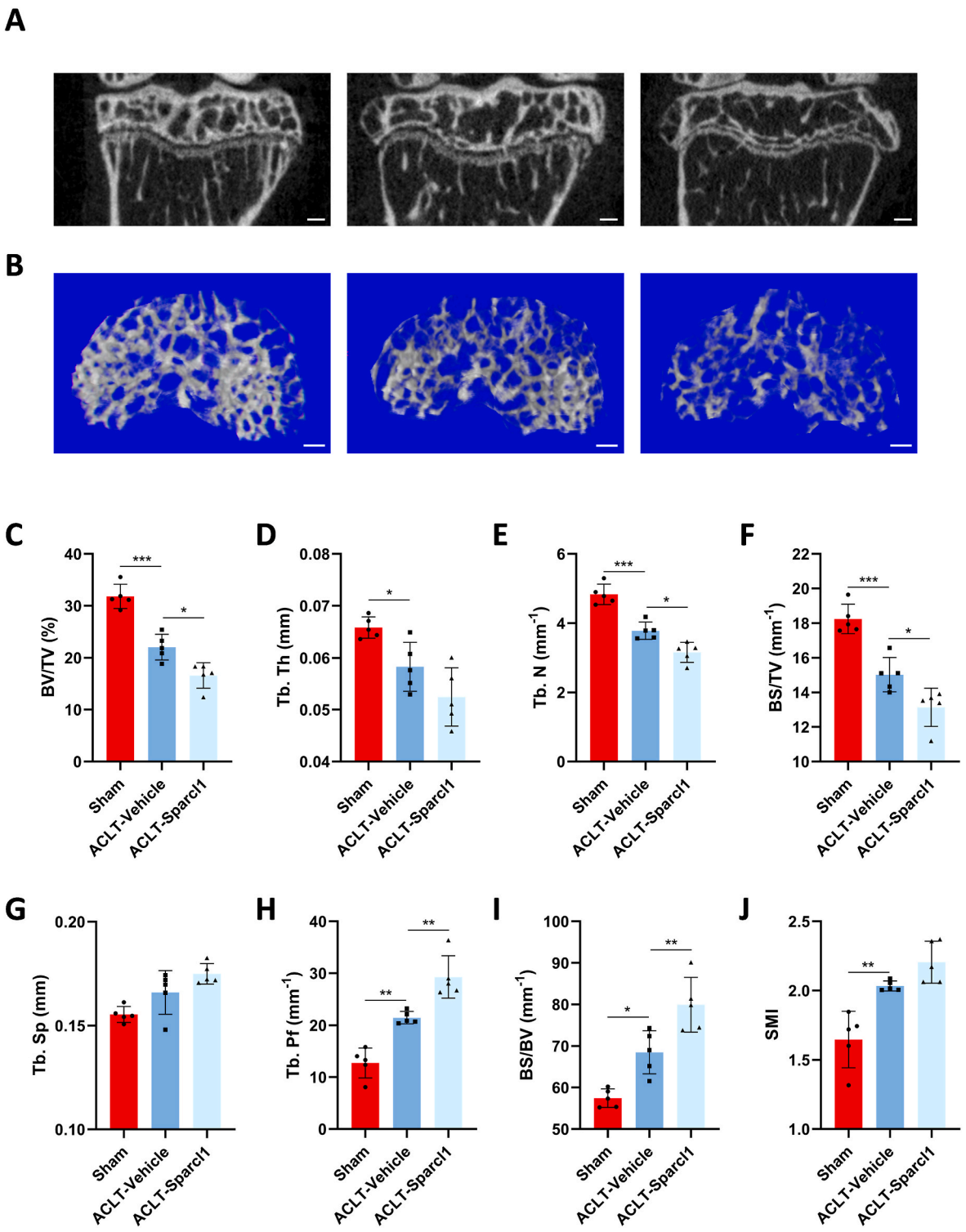

Figure 4. Sparcl1 exacerbated deteriorated subchondral bone in ACLT mice. A Representative micro-CT images of tibial plateau in coronal plane. **B** Representative 3D micro-CT images of subchondral trabecular bone of tibial plateau. **C-J** Quantitative micro-CT analysis of tibial subchondral trabecular bone: BV/TV (C), Tb. th (D), Tb.N (E), BS/TV (F), Tb. sp (G), Tb. Pf (H), BS/BV (I) and SMI (J). BV/TV, Bone Volume/Total Volume; Tb.Th, Trabecular Bone Number; Tb.N, Trabecular Bone Number; BS/TV, Bone Surface/Total Volume; Tb. Sp, Trabecular Bone Separation; Tb. Pf, Trabecular Bone pattern factor; BS/BV, Bone Surface/Bone Volume; SMI, structure model index. n = 5 in each group. Data are expressed as mean ± SD, *P < 0.05; **P < 0.01; ***P < 0.001. One-way ANOVA with post-hoc Bonferroni correction was used for comparisons.

2682), IKKβ (1:1000, Cell Signaling Technology Cat# 2370), SPARCL1 (1:1000, Proteintech Cat#13517-1-AP), β-ACTIN (1:1000, Servicebio Cat# GB11001), Goat Anti-Rabbit IgG (1:5000, Jackson Cat#111–005) and Goat Anti-mouse IgG (1:5000, Jackson Cat#115–005). All the antibody used were commercially available and the information were provided in Supplementary Table 1.

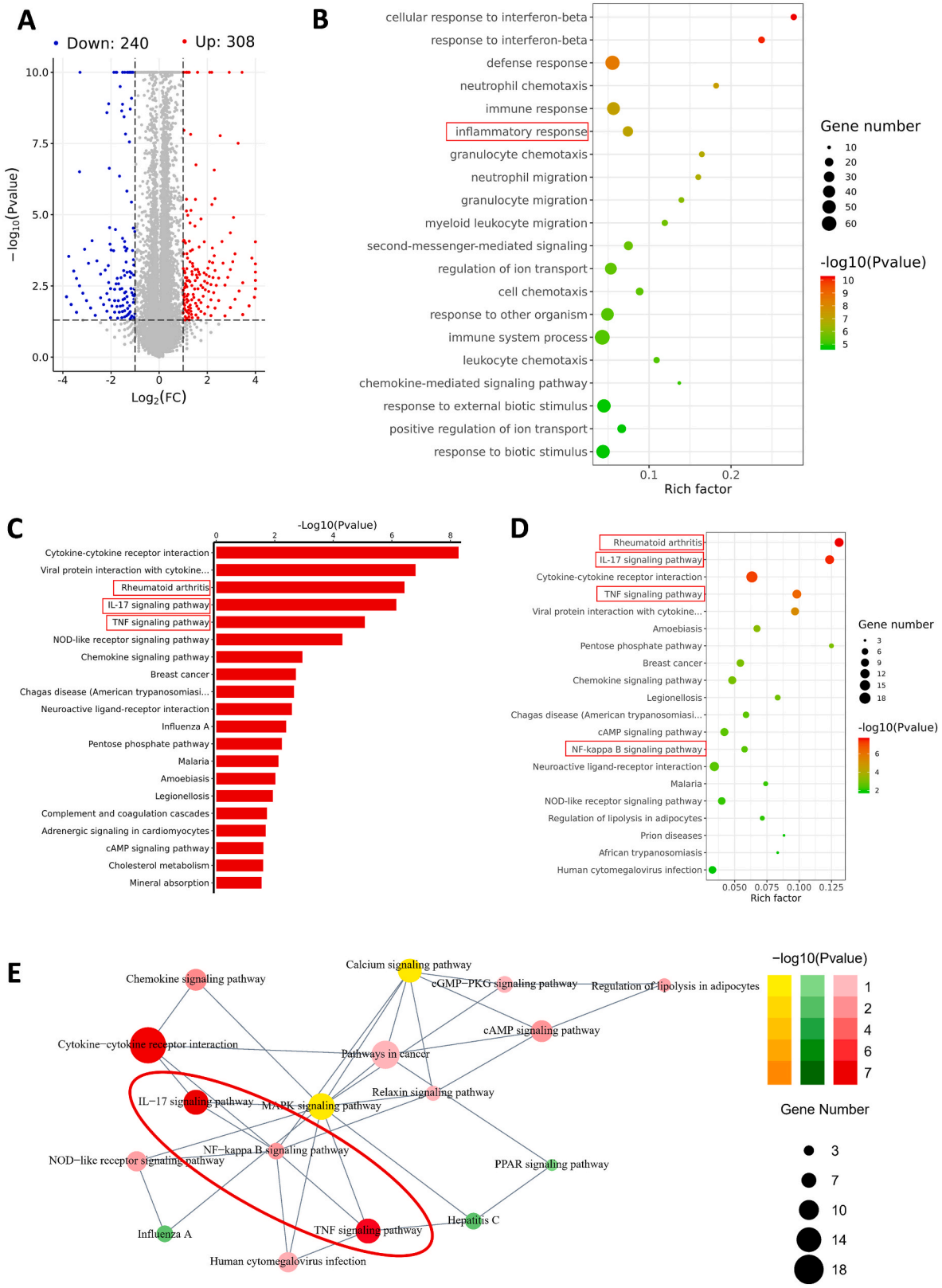

Figure 5. RNA-seq analysis of Sparcl1 treated chondrocytes. A A volcano plot illustrating differentially regulated gene expression from RNA-seq analysis between ctrl and Sparcl1 treated MCCs. Genes upregulated and downregulated are shown in red and blue, respectively. **B** The Gene Ontology (GO) functional clustering of genes in Sparcl1-treated MCC (top 20 most significantly affected categories are shown) **C-D** Kyoto Encyclopedia of Genes and Genomes (KEGG) analysis of total genes (C) and upregulated genes (D) in Sparcl1-treated MCC transcriptome. **E** Pathway network illustrated the relationships of each pathway enriched in KEGG analysis.

2.10. Co-immunoprecipitation (Co-IP)

Co-IP was conducted using Pierce Co-Immunoprecipitation Kit (Thermo) according to the manufacturer's instructions. Briefly, antibody or IgG was coupled to resin by incubating Coupling Buffer and antibody and resin in the spin column for 90–120 min. In this process, cell lysis was prepared. Some of the lysate was retained as input sample. Resin was washed, and mixed with lysis and incubated with gentle mixing overnight at 4 °C. Samples were washed and elution buffer was added in column. The flow-through were collected and analyzed for western blot. The information of reagents used were provided in Supplementary Table 1.

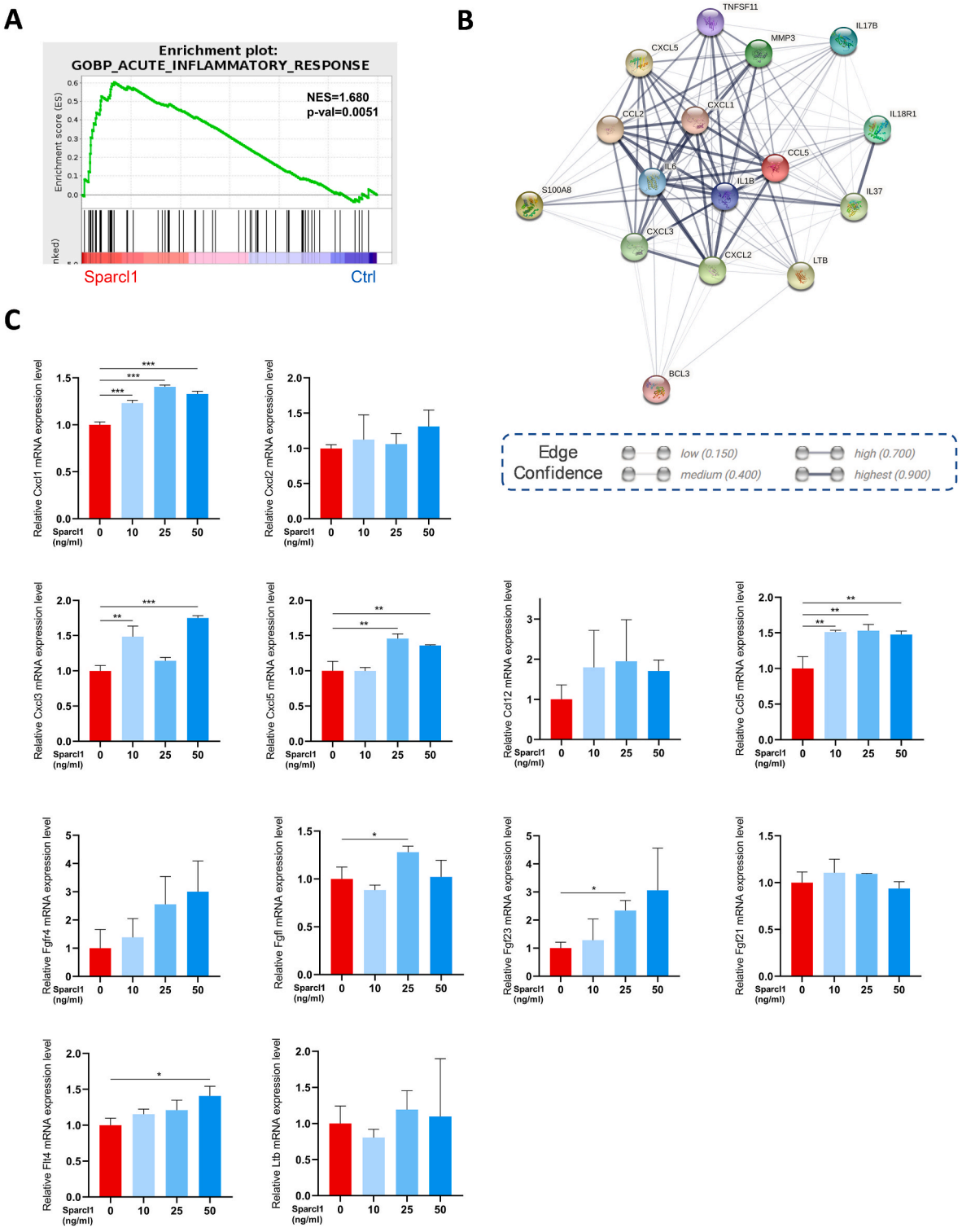

Figure 6. Inflammatory response was increased in Sparcl1 treated chondrocytes. A GSEA plots evaluating the changes of inflammatory response related genes. **B** STRING analysis identified protein–protein interactions in the enriched pathways after Sparcl1 stimulation. **C** Quantification of mRNA levels for DEGs mentioned above in chondrocytes treated with Sparcl1 protein (10, 25, 50 ng/ml). Data are expressed as mean ± SD, *P < 0.05; **P < 0.01; ***P < 0.001. One-way ANOVA with post-hoc Bonferroni correction was used for comparisons.

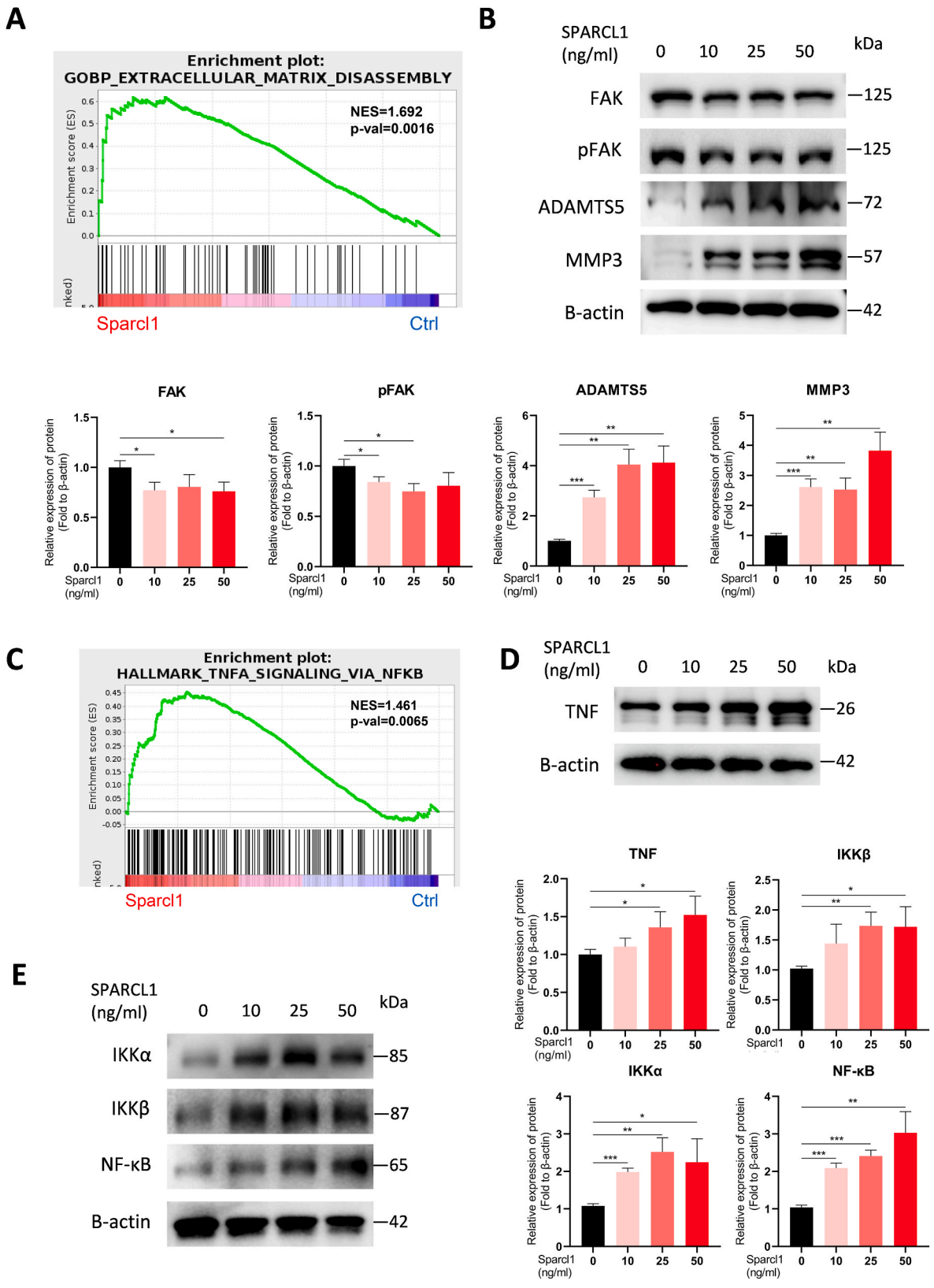

Figure 7. Sparcl1 regulated inflammation and ECM degradation through TNF/NF-κB pathway. A GSEA plots evaluating the changes of ECM disassembly related genes. **B** Protein expression of FAK, pFAK, ADAMTS5 and MMP3 in chondrocytes treated with recombinant Sparcl1 protein (10, 25, 50 ng/ml) for 72 h analyzed by Western blot, and quantification of immunoblots (n = 3). **C** GSEA plots evaluating the changes of TNFA signaling via NF-κB related genes. **D-E** Protein expression of TNF, IKKα, IKKβ, and NF-κB in chondrocytes treated with recombinant Sparcl1 protein (10, 25, 50 ng/ml) for 72 h analyzed by Western blot, and quantification of immunoblots (n = 3). Data are expressed as mean ± SD, *P < 0.05; **P < 0.01; ***P < 0.001. One-way ANOVA with post-hoc Bonferroni correction was used for comparisons.

2.11. RNA extraction, library construction, and sequencing

Total RNA was extracted using the EZ-press RNA Purification Kit according to the manufacturer's protocol. RNA purity and quantification were evaluated using the NanoDrop 2000 spectrophotometer (Thermo Scientific, USA). RNA integrity was assessed using the RNA Nano 6000 Assay Kit of the Bioanalyzer 2100 system (Agilent.

Technologies, CA, USA). A total amount of 3 μg RNA per sample was used as input material for the RNA sample preparations. Sequencing libraries were generated using NEBNext UltraTM RNA Library Prep Kit for Illumina (NEB, USA) following manufacturer's recommendations. The clustering of samples was performed on a cBot Cluster Generation System using TruSeq PE Cluster Kit v3-cBot-HS (Illumia) according to the manufacturer's instructions. After cluster generation, the library preparations were sequenced on an Illumina Novaseq6000 platform and 150 bp paired-end reads were generated. The transcriptome sequencing and analysis were conducted by Shanghai Jiayin Biotechnology Co. ,Ltd. Raw data (raw reads) of fastq format were firstly processed through in-house perl scripts. STAR is used to align clean reads to reference genome [17]. HTSeq v0.6.0 was used to count the reads numbers mapped to each gene. And then FPKM of each gene was calculated based on the length of the gene and reads count mapped to this gene. GO enrichment and KEGG [18] pathway enrichment analysis were performed respectively based on the hypergeometric distribution. GSEA analysis was performed using GSEA software (ver. 4.1.0; Broad Institute, MIT).

2.12. Statistical analysis

All data were expressed as mean ± SD. Statistical analyses were performed with Prism GraphPad. Student's t-test followed by the Tukey–Kramer test was used to evaluate the differences between two groups. Continuous data from the multiple groups were compared using One-way ANOVA with post-hoc Bonferroni correction. $P < 0.05$ was considered statistically different.

3. Results

3.1. The expression of SPARCL1 is elevated in human osteoarthritic articular cartilage

To determine the role of SPARCL1 in OA development, we analyzed RNA sequencing data of the transcriptome of OA cartilage and normal cartilage (GSE113825). GEO database revealed that mRNA level of SPARCL1 was elevated in OA cartilage (Fig. 1A). To further confirm the expression level of SPARCL1 in OA cartilage, we collected 55 pairs of OA cartilage tissues and non-lesion cartilage counterparts. The expression of SPARCL1 protein was evaluated by immunohistochemical staining. Similarly, the results showed that SPARCL1 expression in OA cartilage was significantly higher than that in non-lesion tissues (Fig. 1B–C).

3.2. Sparcl1 induces extracellular matrix degradation in chondrocytes

Extracellular matrix degradation is closely associated with OA progression. Alcian blue staining of micromass showed that proteoglycans in Sparcl1 group was decreased compared to those in the controls (Fig. 2A). In the meantime, according to CCK-8 assay, Sparcl1 showed no significant effect in regulating chondrocyte proliferation (Fig. 2B). Moreover, we found that addition of Sparcl1 reduced the mRNA expression of Aggrecan (Acan), but had no effect on Col2a1 and Sox9 (Fig. 2C). Expression of Mmp3, Mmp13, Adamts1 and Adamts5 were upregulated when treated with Sparcl1 protein (Fig. 2D).

Pro-inflammatory cytokine IL-1β is closely linked with OA occurrence and is usually used to simulate OA in vitro. qPCR results demonstrated that Sparcl1 could promote IL-1β induced ECM degradation and inflammatory response, including downregulation of Col2a1 and upregulation of Mmp3, Mmp13, Ccl2 and IL-6 (Fig. 2E). All these results confirmed that Sparcl1 mediates the degradation of the ECM in chondrocytes.

3.3. Sparcl1 exacerbates OA progression in mice

To examine the function of Sparcl1 on OA development and progression *in vivo*, we performed ACLT surgery in 12-week-old C57/BL6 mice followed with intra-articular administration of recombinant Sparcl1 protein twice a week after surgery. At 6 weeks, all mice were sacrificed and the knees were harvested. Safranin O/fast green staining was used to assess knee joint damage including articular cartilage degradation and synovial tissue hyperplasia (Fig. 3A). As expected, ACLT induced articular cartilage degeneration and synovial thickening. The ACLT + Sparcl1 group showed more severe cartilage erosion and synovial hyperplasia compared with the vehicle group, evidenced by markedly higher OARSI scores and synovitis scores in Sparcl1 group (Fig. 3B–C). Micro-CT showed obvious osteophyte formation in the vehicle group (Fig. 2D), in the aspects of osteophyte size and maturity. Although it was not statistically significant, Sparcl1 injection promoted osteophyte formation (Fig. 3E–F).

Moreover, micro-CT illustrated that Sparcl1 could accelerate subchondral trabecular bone deterioration after ACLT surgery compared with the vehicle group (Fig. 4A–B). BV/TV, Tb.Th, Tb.N, and BS/TV showed obvious decline tendency compared to the vehicle group, among which the change of BV/TV, Tb.N and BS/TV were statistically significant (Fig. 4C–F). Meanwhile, we also found the values of Tb. Pf and BS/BV were increased when treated with Sparcl1. Tb. Sp and SMI were slightly enhanced with no statistical significance (Fig. 4G–J).

3.4. RNA-seq analysis indicates Sparcl1 activates inflammation and ECM degradation

To further analyze how Sparcl1 mediated ECM degradation, we conducted RNA-sequencing in chondrocytes treated with recombinant Sparcl1 protein. Addition of Sparcl1 resulted in the upregulation of 308 genes and downregulation of 240 genes (Fig. 5A). Gene ontology (GO) analysis showed that Sparcl1 showed significantly influence on the inflammatory response (Fig. 5B). KEGG pathway analysis showed rheumatoid arthritis, IL-17 signaling pathway and TNF signaling pathway were enriched (Fig. 5C). Besides, NF-κB signaling pathway was also enriched in upregulated genes (Fig. 5D). Furthermore, pathway network analysis revealed that TNF, NF-κB and IL-17 signaling pathway were closely related to each other and were the centre part of this pathways (Fig. 5E).

As we know, rheumatoid arthritis, TNF signaling pathway, IL-17 signaling pathway and NF-κB signaling pathway were all related with inflammation and ECM degradation. Meanwhile, GESA analysis also confirmed that acute inflammatory response was obviously activated (Fig. 6A). Thus, to further elucidate the molecular mechanism of genes in the categories described above, we introduced these genes into the STRING (https://string-db.org/) database to construct the protein–protein interaction network. It was demonstrated that these genes are closely clustered together and form a complex network (Fig. 6B). We then confirmed the expression level of these genes when chondrocytes were treated with various concentrations of Sparcl1 proteins. Mmp3 (Fig. 2D) Cxcl1, Cxcl3, Cxcl5, Ccl5, Fgfl, Fgf23 and Flt4 were significantly increased, while Cxcl2, Ccl12, Fgfr4, Fgf21 and Ltb showed nonsignificant increasement (Fig. 6C). Accordingly, these data confirmed the effect of Sparcl1on inflammatory response and indicated that TNF/NF-κB signaling pathway might be the underlying pathway.

3.5. Sparcl1 regulates ECM degradation through TNF/NF-κB signaling pathway

According to GESA analysis, ECM disassembly related genes were obviously upregulated after treatment with Sparcl1 (Fig. 7A). In the

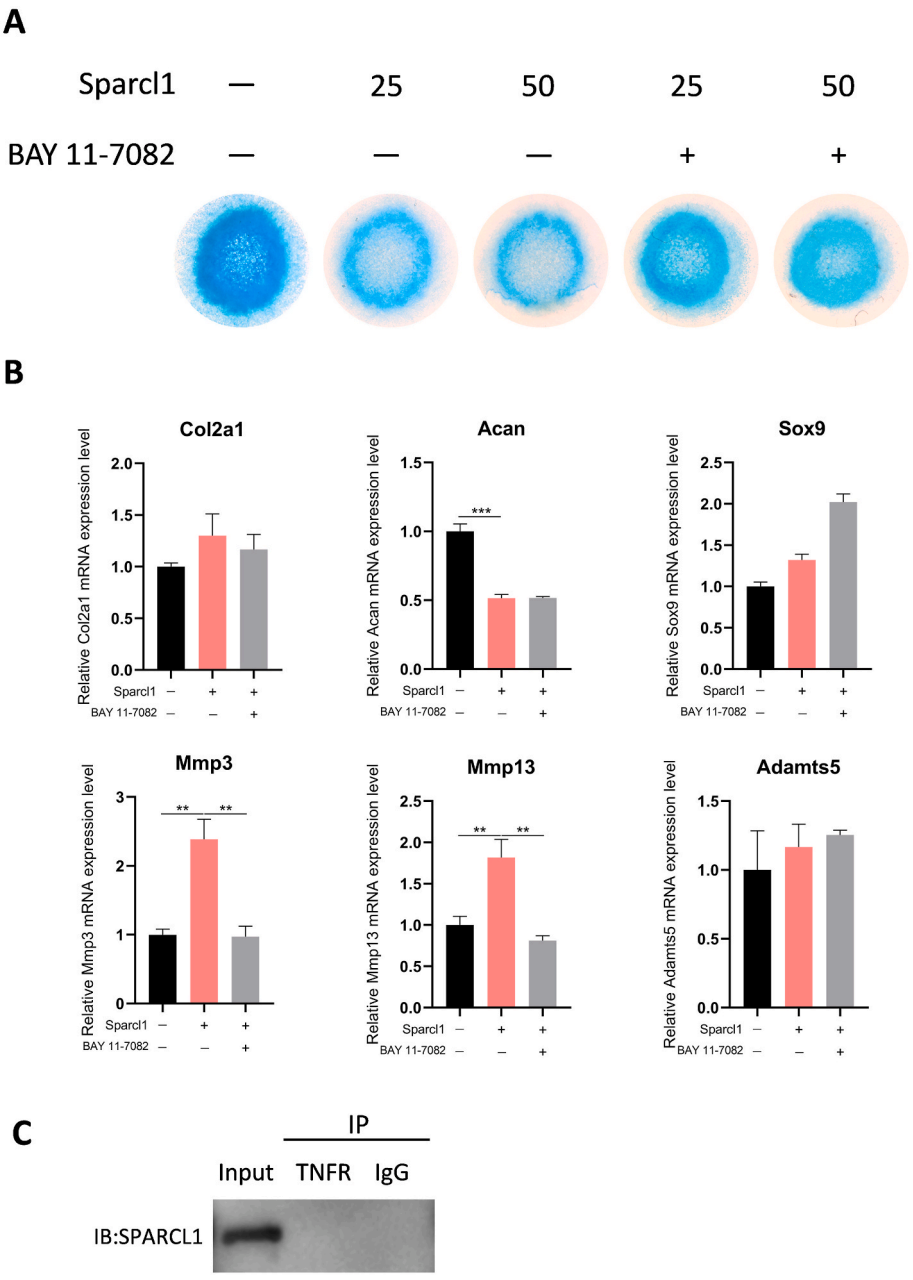

Figure 8. BAY 11–7082 could reverse Sparcl1 induced ECM degradation and related gene expression. A Alcian blue staining of ATDC5 with micromass culture in chondrogenesis media with or without recombinant Sparcl1 protein and BAY 11–7082 (2.5 μM). Representative image of staining at day 8 is shown. **B** Quantification of mRNA levels for Col2a1, Acan, Sox9, Mmp3, Mmp13, Adamts5 in MCC treated with recombinant Sparcl1 protein (50 ng/ml) and BAY 11–7082 (2.5 μM) for 48 h. **C** Immunoblot analysis of MCC, immunoprecipitated with anti-TNFR and IgG and analyzed by immunoblot with anti-SPARCL1.

meantime, except for regulating ECM, Sparcl1 is also known as an adhesion molecule. Therefore, we explored adhesion related proteins and catabolic markers of chondrocyte via western blot. The results demonstrated that Sparcl1 increased the expression of ADAMTS5 and MMP3. Focal adhesion related proteins FAK and pFAK (Phos-FAK) were decreased, which indicated that Sparcl1 could impair cell focal adhesion (Fig. 7B). GSEA analysis also identified that TNF/NF-κB signaling pathway was obviously activated (Fig. 7C). Immunoblot results showed that TNF, IKKα, IKKβ and NF-κB were upregulated (Fig. 7D–E).

When we inhibited TNF/NFκB signaling pathway by BAY 11–7082, which is an IκBα phosphorylation and NF-κB inhibitor, micromass experiments showed that ECM degradation induced by Sparcl1 was reversed (Fig. 8A). Furthermore, expression of downstream cartilage catabolism-related genes which were upregulated by Sparcl1, such as Mmp3 and Mmp13, were decreased by the addition of BAY 11–7082 (Fig. 8B). However, BAY 11–7082 showed little effects on cartilage anabolism-related genes, such as Col2a1, Acan and Sox9 (Fig. 8B). Co-IP results showed that Sparcl1 was not directly bound to TNFR, which implied the important role of TNF in activating the downstream signaling pathway (Fig. 8C). All these results indicated that Sparcl1 regulates ECM degradation through TNF/NFκB pathway.

4. Discussion

OA is the most common form of arthritis characterized by progressive degeneration of the articular cartilage. ECM is one of the first pathogenesis during the progression of OA [19,20]. Due to the protective function of ECM, extensive studies focused on the mechanism of

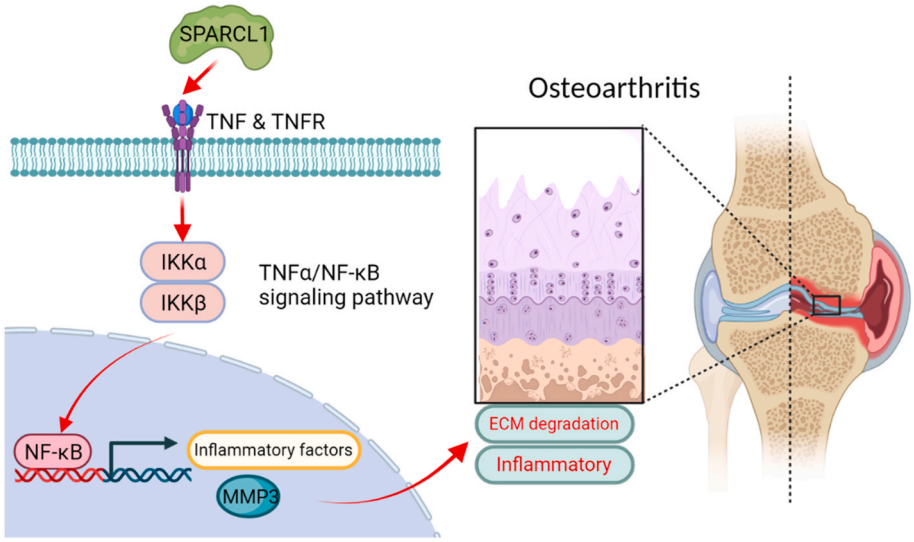

Figure 9. Mechanism of Sparcl1 in exacerbate osteoarthritis. Diagram illustrating the mechanism how Sparcl1 influences OA pathogenesis through the TNF/NFκB signaling pathway.

ECM degradation or maintenance of ECM homeostasis as a treatment target [21–24]. However, molecular mechanisms of ECM degradation in OA are still poorly understood. RNA microarray study found that SPARCL1 expression was elevated in OA meniscus [16], but its expression is still not clear in OA cartilage. In the current study, we focused on the function of SPARCL1, a matricellular protein, in OA cartilage and examined how SPARCL1 promotes OA progression. Through GEO database and cartilage specimen IHC results, we noticed that SPARCL1 expression was elevated in OA cartilage. *In vitro* experiments revealed that recombinant Sparcl1 protein could inhibit ECM generation and expression of some cartilage anabolism-related gene (Acan), but promote the expression of catabolism-related genes (Mmp3, Mmp13, Adamts1, Adamts5). Importantly, intra-articular injection of recombinant Sparcl1 protein also accelerated OA progression *in vivo*. Mechanically, RNA-Seq analysis revealed that Sparcl1 could enhance inflammatory response. OA and inflammation related gene sets, such as rheumatoid arthritis, IL-17 signaling pathway, TNF signaling pathway and NF-κB signaling pathway, were also enriched. Related DEGs (differential expressed genes) were confirmed and expression of IKKα, IKKβ and NF-κB was also elevated. ECM degradation and expression alternation of related genes which were induced by Sparcl1, could be reversed when the TNF/NF-kB signaling pathway is inhibited. Accordingly, these data illustrated that SPARCL1 promotes ECM degradation and inflammation in OA via TNF/NF-κB signaling pathway (Fig. 9).

Up to now, studies on SPARCL1 are very limited. In previous studies, SPARCL1 has been reported as an antagonist of cell adhesion to the underlying substratum [8,25]. Girard et al. found that SPARCL1 could inhibit endothelial cell attachment and adhesion, and reduce the ability to form focal adhesions [25]. Identically, SPARCL1 has been demonstrated to provide de-adhesive effects and characterized as anti-proliferative factors in distinct cellular contexts [26]. In addition, SPARCL1 has been reported to be downregulated in many human epithelial cancers, such as non-small-cell lung cancer [27], prostate cancer [28], colon cancer [29] and gastric cancer [30]. SPARCL1 could inhibit the migration and invasion of cancers [31,32]. Our results also showed that SPARCL1 could downregulate the expression of FAK and its phosphorylation. However, cellular adhesion was not ranked in GO or KEGG analysis, indicating that it might not be the critical reason for ECM degradation in chondrocytes.

RNA-Seq results and known upstream of ECM degradation indicated that SPARCL1 would take effect through the TNF/NF-κB pathway. The TNF/NF-κB signaling pathway is a relatively thoroughly investigated pathway [33]. TNF and NF-κB studies have long been closely associated, and many biological effects of TNF are actually mediated by NF-κB [33]. The inhibitor of nuclear factor kappa B kinase (IKK) complex, including IKKα and IKKβ, could lead to NF-κB phosphorylation and nuclear translocation, resulting in the transcription of downstream target genes [34,35]. We discovered that Sparcl1 could activate IKKα and IKKβ, leading to the increased expression of NF-κB. ECM degradation related genes, such as MMP3, and many inflammatory factors, were the downstream effectors of NF-κB. Nevertheless, considering that the basic function of SPARCL1 is regulating adhesion, which also contributes to ECM homeostasis in OA, it is difficult to deny the de-adhesion role of SPARCL1 in promoting TNF activation [36,37]. To the best of our knowledge, the present study is the first to report the potential relationship between SPARCL1 and TNF/NF-κB pathway.

At present, there are still some limitations and unsolved problems about the role of SPARCL1 in OA pathogenesis and development in this study. One of the limitations is the lack of a large cohort to analyze SPARCL1 expression level at different stages of OA. Especially the expression level of SPARCL1 in the early stage of OA, which is crucial for exploring how SPARLC1 is regulated in OA initiation. It is also unclear whether the expression of SPARC, the family member and homolog of SPARCL1, is simultaneously altered in OA cartilage. It was reported that both SPARC and SPARCL1 could be cleaved by specific members of MMP family. In particular, SPARCL1 could be cleaved by MMP3, with the consequent release of a shorter C-terminal fragment, known as 'SPARC-like fragment' (SLF), which was reported to functionally oppose full-length SPARCL1 [38,39]. Therefore, how these three proteins, MMP3, SPARCL1 and SPARC, regulating each other, is quite complicated and might be important to further elucidate the mechanism of SPARCL1 in OA progression. Moreover, how Sparcl1 activates TNF/NF-κB is still unknow and remains to be further studied. Hence, further investigations on the role and underlying mechanism of SPARCL1 in OA is warranted in future studies.

In conclusion, SPARCL1 expression is elevated in OA cartilage. SPARCL1 could accelerate OA progression by promoting ECM degradation and inflammatory response via TNF/NF-κB pathway. This study may help to gain further insights into the underlying molecular mechanism in OA development, which could contribute to the development of disease-modifying treatments for OA.

Funding

This work was supported by the Basic Science Program of Shanghai Jiao Tong University Affiliated Sixth People's Hospital (Grant no. ynms202102, ynqn202302), National Natural Science Fund of China (82302750), Shanghai "Science and Technology Innovation Action Plan" domestic science and technology cooperation project (Grant no. 20025800200), the Interdisciplinary Program of Shanghai Jiao Tong University (Grant no. YG2019QNB16).

Data and code availability

RNA-Seq raw data reported in this paper have been deposited in the Gene Expression Omnibus database under accession number GSE210743.

CRediT authorship contribution statement

Yu Miao: Conceptualization, Methodology, Validation, Formal analysis, Investigation, Data curation, Writing – original draft, Writing – review & editing, Visualization. **Shenghui Wu:** Methodology, Validation, Formal analysis, Visualization. **Ziling Gong:** Visualization, Funding acquisition, this research did not receive any specific grant from funding agencies in the public, commercial, or not-for-profit sectors. All authors saw and approved a final version of the manuscript before submission. **Yiwei Chen:** Methodology, Formal analysis. **Feng Xue:** Methodology, Validation, Resources. **Kexin Liu:** Methodology, Resources. **Jian Zou:** Resources. **Yong Feng:** Conceptualization, Writing – review & editing, Supervision, Project administration. **Guangyi Li:** Conceptualization, Writing – review & editing, Supervision, Project administration.

Declaration of AI and AI-assisted technologies in the writing process

The authors declare that no AI and AI-assisted technologies have been used in the writing process.

Declaration of competing interest

The authors declare that they have no conflicts of interest.

Appendix A. Supplementary data

Supplementary data to this article can be found online at https://doi.org/10.1016/j.jot.2024.02.009.

References

[1] Glyn-Jones S, Palmer AJ, Agricola R, Price AJ, Vincent TL, Weinans H, et al. Osteoarthritis. Lancet 2015;386:376–87.
[2] Blagojevic M, Jinks C, Jeffery A, Jordan KP. Risk factors for onset of osteoarthritis of the knee in older adults: a systematic review and meta-analysis. Osteoarthritis Cartilage 2010;18:24–33.
[3] Hunter DJ, Bierma-Zeinstra S. Osteoarthritis. Lancet 2019;393:1745–59.
[4] Little CB, Hunter DJ. Post-traumatic osteoarthritis: from mouse models to clinical trials. Nat Rev Rheumatol 2013;9:485–97.
[5] Shi Y, Hu X, Cheng J, Zhang X, Zhao F, Shi W, et al. A small molecule promotes cartilage extracellular matrix generation and inhibits osteoarthritis development. Nat Commun 2019;10:1914.
[6] Miao Y, Chen Y, Xue F, Liu K, Zhu B, Gao J, et al. Contribution of ferroptosis and GPX4's dual functions to osteoarthritis progression. EBioMedicine 2022;76:103847.
[7] Husa M, Liu-Bryan R, Terkeltaub R. Shifting HIFs in osteoarthritis. Nat Med 2010;16:641–4.
[8] Sullivan MM, Sage EH. Hevin/SC1, a matricellular glycoprotein and potential tumor-suppressor of the SPARC/BM-40/Osteonectin family. Int J Biochem Cell Biol 2004;36:991–6.
[9] Cheng X, Chen X, Zhang M, Wan Y, Ge S, Cheng X. Sparcl1 and Atherosclerosis. J Inflamm Res 2023;16:2121–7.
[10] Zhang HP, Wu J, Liu ZF, Gao JW, Li SY. SPARCL1 is a novel prognostic Biomarker and Correlates with tumor microenvironment in colorectal cancer. BioMed Res Int 2022;2022:1398268.
[11] Gagliardi F, Narayanan A, Mortini P. SPARCL1 a novel player in cancer biology. Crit Rev Oncol Hematol 2017;109:63–8.
[12] Ye H, Wang WG, Cao J, Hu XC. SPARCL1 suppresses cell migration and invasion in renal cell carcinoma. Mol Med Rep 2017;16:7784–90.
[13] Ma Y, Xu Y, Li L. SPARCL1 suppresses the proliferation and migration of human ovarian cancer cells via the MEK/ERK signaling. Exp Ther Med 2018;16:3195–201.
[14] Zhao SJ, Jiang YQ, Xu NW, Li Q, Zhang Q, Wang SY, et al. SPARCL1 suppresses osteosarcoma metastasis and recruits macrophages by activation of canonical WNT/β-catenin signaling through stabilization of the WNT-receptor complex. Oncogene 2018;37:1049–61.
[15] Wang Y, Liu S, Yan Y, Li S, Tong H. SPARCL1 promotes C2C12 cell differentiation via BMP7-mediated BMP/TGF-β cell signaling pathway. Cell Death Dis 2019;10:852.
[16] Brophy RH, Zhang B, Cai L, Wright RW, Sandell LJ, Rai MF. Transcriptome comparison of meniscus from patients with and without osteoarthritis. Osteoarthritis Cartilage 2018;26:422–32.
[17] Dobin A, Davis CA, Schlesinger F, Drenkow J, Zaleski C, Jha S, et al. STAR: ultrafast universal RNA-seq aligner. Bioinformatics 2013;29:15–21.
[18] Kanehisa M, Araki M, Goto S, Hattori M, Hirakawa M, Itoh M, et al. KEGG for linking genomes to life and the environment. Nucleic Acids Res 2008;36:D480–4.
[19] Guilak F, Nims RJ, Dicks A, Wu CL, Meulenbelt I. Osteoarthritis as a disease of the cartilage pericellular matrix. Matrix Biol 2018;71-72:40–50.
[20] Heinegard D, Saxne T. The role of the cartilage matrix in osteoarthritis. Nat Rev Rheumatol 2011;7:50–6.
[21] Vincent TL, McClurg O, Troeberg L. The extracellular matrix of articular cartilage controls the Bioavailability of pericellular matrix-bound growth factors to drive tissue homeostasis and Repair. Int J Mol Sci 2022;23(11).
[22] Zhang Y, Hou M, Liu Y, Liu T, Chen X, Shi Q, et al. Recharge of chondrocyte mitochondria by sustained release of melatonin protects cartilage matrix homeostasis in osteoarthritis. J Pineal Res 2022:e12815.
[23] McClurg O, Tinson R, Troeberg L. Targeting cartilage degradation in osteoarthritis. Pharmaceuticals 2021;14.
[24] Kwak JS, Lee Y, Yang J, Kim SK, Shin Y, Kim HJ, et al. Characterization of rhodanine derivatives as potential disease-modifying drugs for experimental mouse osteoarthritis. Osteoarthritis Cartilage 2022.
[25] Girard JP, Springer TA. Modulation of endothelial cell adhesion by hevin, an acidic protein associated with high endothelial venules. J Biol Chem 1996;271:4511–7.
[26] Framson PE, Sage EH. SPARC and tumor growth: where the seed meets the soil? J Cell Biochem 2004;92:679–90.
[27] Bendik I, Schraml P, Ludwig CU. Characterization of MAST9/Hevin, a SPARC-like protein, that is down-regulated in non-small cell lung cancer. Cancer Res 1998;58:626–9.
[28] Xiang Y, Qiu Q, Jiang M, Jin R, Lehmann BD, Strand DW, et al. SPARCL1 suppresses metastasis in prostate cancer. Mol Oncol 2013;7:1019–30.
[29] Naschberger E, Liebl A, Schellerer VS, Schutz M, Britzen-Laurent N, Kolbel P, et al. Matricellular protein SPARCL1 regulates tumor microenvironment-dependent endothelial cell heterogeneity in colorectal carcinoma. J Clin Invest 2016;126:4187–204.
[30] Li P, Qian J, Yu G, Chen Y, Liu K, Li J, et al. Down-regulated SPARCL1 is associated with clinical significance in human gastric cancer. J Surg Oncol 2012;105:31–7.
[31] Hu H, Zhang H, Ge W, Liu X, Loera S, Chu P, et al. Secreted protein acidic and rich in cysteines-like 1 suppresses aggressiveness and predicts better survival in colorectal cancers. Clin Cancer Res 2012;18:5438–48.
[32] Hurley PJ, Marchionni L, Simons BW, Ross AE, Peskoe SB, Miller RM, et al. Secreted protein, acidic and rich in cysteine-like 1 (SPARCL1) is down regulated in aggressive prostate cancers and is prognostic for poor clinical outcome. Proc Natl Acad Sci U S A 2012;109:14977–82.
[33] Hayden MS, Ghosh S. Regulation of NF-kappaB by TNF family cytokines. Semin Immunol 2014;26:253–66.
[34] Hayden MS, Ghosh S. Shared principles in NF-kappaB signaling. Cell 2008;132:344–62.
[35] Oeckinghaus A, Hayden MS, Ghosh S. Crosstalk in NF-kappaB signaling pathways. Nat Immunol 2011;12:695–708.
[36] Legerstee K, Houtsmuller AB. A layered View on focal adhesions. Biology 2021;10(11).
[37] Urciuoli E, Peruzzi B. Involvement of the FAK network in Pathologies related to altered Mechanotransduction. Int J Mol Sci 2020;21(24).
[38] Kucukdereli H, Allen NJ, Lee AT, Feng A, Ozlu MI, Conatser LM, et al. Control of excitatory CNS synaptogenesis by astrocyte-secreted proteins Hevin and SPARC. Proc. Natl. Acad. Sci. U.S.A 2011;108:E440–9.
[39] Weaver M, Workman G, Schultz CR, Lemke N, Rempel SA, Sage EH. Proteolysis of the matricellular protein hevin by matrix metalloproteinase-3 produces a SPARC-like fragment (SLF) associated with neovasculature in a murine glioma model. J Cell Biochem 2011;112:3093–102.